Peer-reviewed version available at Metals 2018, 8, 469; doi:10.3390/met8060469

Article

Techno-economic analysis of high-pressure metal hydride compressor systems

Claudio Corgnale*, Martin Sulic

Greenway Energy, 301 Gateway Drive, Aiken, SC (USA), 29803
* Correspondence: claudio.corgnale@greenway-energy.com; Tel.: +1-803-617-9689

Abstract: Traditional high pressure mechanical compressors account for over half of the car station's cost, have insufficient reliability and are not feasible for a large-scale fuel cell market. An alternative technology, employing a two-stage, hybrid system based on electrochemical and metal hydride compression technologies, represents an excellent alternative to conventional compressors. The high-pressure stage, operating at 100-875 bar, is based on a metal hydride thermal system. A techno-economic analysis of the metal hydride system is presented and discussed. A model of the metal hydride system was developed, integrating a lumped parameter mass and energy balance model with an economic model. A novel metal hydride heat exchanger configuration is also presented, based on mini-channel heat transfer systems, allowing for effective high-pressure compression. Several metal hydrides were analyzed and screened, demonstrating that one selected material, namely $(Ti_{0.97}Zr_{0.03})_{1.1}Cr_{1.6}Mn_{0.4}$, is likely the best candidate material to be employed for high-pressure compressors under the specific conditions. System efficiency and costs were assessed based on the properties of currently available materials at industrial levels. Results show that the system can reach pressures on the order of 875 bar with thermal power provided at approximately 150 °C. The system cost is comparable with the current mechanical compressors and can be reduced in several ways as discussed in the paper.

Keywords: High pressure hydrogen; Metal hydride-based high pressure compression; Techno-economic analysis; Ti-based AB_2 metal hydrides; Mini-channel heat exchanger

1. Introduction

One of the main hurdles to be overcome for a large-scale hydrogen economy is relative to the H_2 delivery. The United States Department of Energy (DOE) has essentially identified three approaches to transport and delivery hydrogen at large scale [1]. Each of the scenarios requires the presence of high pressure hydrogen systems. Currently DOE set its fueling pressure targets at approximately 875 bar, with inlet hydrogen at about 100 bar, and with flow rates up to 100 kg/h [1]. Among the other targets for hydrogen compression systems, DOE identified the uninstalled cost target for the FY 2020 at 275,000 $, the energy requirement at 1.6 kWh/kg, availability equal to 85% and annual maintenance cost equal to 4% of the uninstalled cost[1] [1]. Currently, mechanical compressors cannot achieve the DOE targets and have several additional drawbacks working at the specified operating conditions. Valid alternative processes are represented by hybrid systems comprised of electrochemical compression (EHC) systems, operating at lower pressures (10-100 bar), integrated with thermal compression systems, operating at pressures on the order of 100-875 bar. One of the main advantages of a hybrid system over other alternative solutions is in the possibility of recovering the available waste heat from the EHC to pressurize and discharge the hydrogen from the thermal compression system, based on metal hydrides. The work presented here focuses on the high-pressure metal hydride-based compression system. Metal hydride materials absorb hydrogen through an

[1] The targets are for: inlet pressure of 100 bar, hydrogen flow rate of 100 kg/h [1]

Peer-reviewed version available at Metals 2018, 8, 469; doi:10.3390/met8060469

exothermic chemical reaction and release the absorbed hydrogen reversibly, through an endothermic chemical reaction. The chemical reaction equilibrium pressures are direct functions of the operating temperatures. Therefore, hydrogen can be absorbed in the materials at low temperatures and corresponding low pressures. By providing high temperature thermal power, the hydrogen can be released at high pressure without the use of external electric power.

A comprehensive review of the available MH materials, heat transfer and pressure vessel concepts, operating at maximum pressures on the order of 600-700 bar, can be found in Reference [2]. Currently, available MHs for high pressure hydrogen compression are Ti-based materials (laves phase, or AB_2 phase materials). Depending on the material formulation, MH compressors can achieve pressures on the order of 800-900 bar at temperatures on the order of 120-150 °C without any electric input [3-4]. Recent research and development work focused on the design of high pressure MH-based compression systems, examining the technical performance of the proposed material heat exchanger coupled solutions. Gkanas et al. [5] propose the use of a two-stage metal hydride compression system to achieve maximum pressure ratios of 22, with a maximum delivery pressure of 320 bar at 130 °C. The first stage material is an AB_5 alloy, namely $LaNi_5$, while the second stage material is an AB_2 type material based on Zr-V-Mn-Nb. Karagiorgis et al [6] investigate the use of MH materials to compress hydrogen, using waste heat available at temperatures in the range 10 – 80 °C. Maximum compression ratios of about 32 were achieved, compressing hydrogen between 7 bar and 220 bar. However, the system is comprised of 6 stage metal hydride compressors, using AB_5 and AB_2 materials. Galvis et al. [7] also analyze the use of a three stage MH compressor, comprised of AB_2 type materials (Ti-Zr-Cr-Mn-V), to achieve an overall compression ratio of about 82. The system was designed to reach a pressure of 115 bar, with inlet pressure of 1.4 bar, with maximum desorption temperature of 100 °C. None of the proposed systems was designed for pressures on the order of 875 bar, as required by the DOE targets and, consequently, the techno-economic feasibility of systems achieving very high pressures was never examined.

The present work describes a techno-economic model applied to candidate high pressure metal hydride materials for high pressure hydrogen compression. The model includes lumped parameter steady state mass and energy balance equations, integrated with an economic model. The technical performance of the overall material-heat exchanger system was assessed and discussed, proposing a novel heat transfer system model, based on mini-channel cylindrical tubes heat exchangers. The potential of available materials to meet the targets is also discussed, with proposed solutions to enhance the economic performance.

2. The hybrid hydrogen compressor concept

A two-stage hybrid compressor system is proposed, as an alternative to conventional mechanical compressors, for efficient and low cost high-pressure hydrogen compression systems. A simplified schematic of the proposed concept is shown in Figure 1. The first stage is based on an electrochemical system, referred to as 'Low pressure EHC'. The second stage is a pure thermal compression system, based on metal hydride materials, referred to as 'High pressure MHC'.

The EHC stage operates at manometric compression ratios on the order of 10, compressing the hydrogen from an inlet pressure of 10 bar up to approximately 100 bar. Molecular hydrogen is oxidized at the anode of an electrochemical system producing protons and electrons. The protons are driven through a proton exchange membrane and combined with electrons at the cathode to deliver high-pressure hydrogen. The outlet pressure is maintained at relatively low values (100 bar) in order to minimize hydrogen back diffusion across the membrane. The inlet hydrogen flow needs to be humidified to operate the electrochemical compression effectively using traditional Nafion® membranes. A dryer unit at the exit of the first stage compressor separates the compressed gas from the water, which is collected in a liquid tank unit. The water is recirculated in the humidification unit to assure the right level of humidity in the electrochemical system. The hydrogen at the exit of the first stage is stored in a buffer tank to assure a continuous flow in the thermal stage of the system. The second stage (MHC stage) of the hybrid system operates at higher pressures with the objective of achieving pressures on the order of 875 bar as required by the DOE targets. This stage is comprised

Preprints (www.preprints.org) | NOT PEER-REVIEWED | Posted: 4 June 2018 doi:10.20944/preprints201806.0025.v1

Peer-reviewed version available at Metals 2018, 8, 469; doi:10.3390/met8060469

of a thermal compression system, based on MH materials. Such materials absorb hydrogen through an exothermic chemical reaction and release the absorbed hydrogen reversibly, through an endothermic chemical reaction. The equilibrium pressures for the chemical reactions are a direct function of their operating temperatures. Therefore, hydrogen can be absorbed at low temperatures and pressures and, by providing higher temperature thermal power during the desorption process, the hydrogen pressure can be increased without the use of any external electric power.

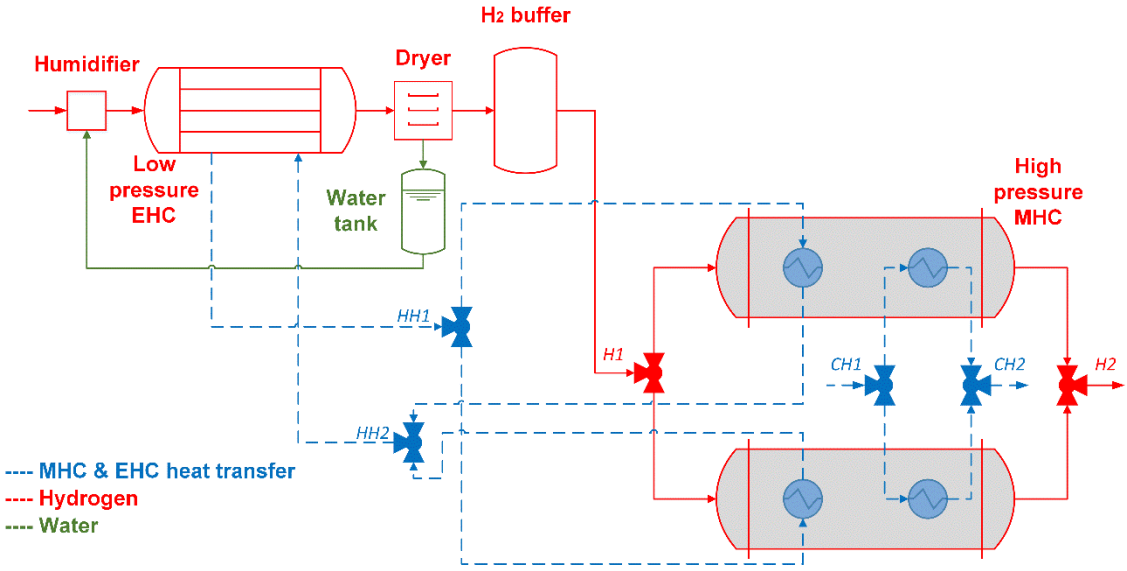

Figure 1. Hybrid EHC/MHC system concept.

Each metal hydride unit intrinsically operates in a batch (or discontinuous) mode, either in hydrogen charging mode or in hydrogen release mode. Therefore, to assure steady hydrogen flow, at least two parallel metal hydride units need to be coupled in series with the electrochemical unit (Figure 1). One of the main advantages of the proposed solution over competing approaches (e.g. pure thermal compressor or pure electrochemical system) is the possibility of recovering the EHC waste heat to feed the thermal MH system during hydrogen desorption, as shown in Figure 1. This substantially increases the overall system efficiency [3]. The point HH1 identifies the inlet condition of the hot utility (i.e. from the EHC) heat transfer fluid, while the HH2 point represents the corresponding outlet condition, after hydrogen desorption in the MHC unit. The waste heat from the EHC unit is available at temperatures on the order of 150-160 °C. The hydrogen is charged in the MHC system using external cold utility (i.e. water at temperature on the order of 10-15 °C) heat transfer. The points CH1 and CH2 in Figure 1 represent the inlet and outlet points of the cold utility fluid, respectively. Depending on the EHC membrane selection and on the MHC material choice, the system has the potential to achieve a complete EHC waste heat recovery without the need for external thermal power input [3].

More information on the overall system and on the EHC stage characteristics, especially relative to the energy integration with the MHC stage, can be found elsewhere [3]. The attention of the work discussed in the current document was paid on the high pressure thermal compression unit, examining the techno-economic performance of the MH systems.

3. The techno-economic analysis model

A simplified lumped parameter techno-economic model was developed to assess the performance of the high-pressure MH compression system.

3.1. Metal hydride compressor system technical performance model

Peer-reviewed version available at Metals 2018, 8, 469; doi:10.3390/met8060469

The metal hydride system model includes steady state lumped parameters mass and energy balance equations. With reference to Figure 1, the mass balance equation of the MHC stage is expressed as:

$$\dot{m}_{H1} = \dot{m}_{H2} \tag{1}$$

Equation 1 is valid assuming continuity of operation and represents the steady state balance of mass for the MHC system. The hydrogen flow is split between the two parallel metal hydride units.

The lumped parameter steady state energy balance equation is expressed as:

$$\begin{aligned} \dot{m}_{H2}h_{H2} - \dot{m}_{H1}h_{H1} &= \frac{(M_{MH}\overline{C_{PMH}} + M_W\overline{C_{PW}})(T_{des} - T_{abs})}{\Delta t_{des}} + \dot{m}_{H2}\Delta H_{des} \\ &- \frac{(M_{MH}\overline{C_{PMH}} + M_W\overline{C_{PW}})(T_{des} - T_{abs})}{\Delta t_{abs}} + \dot{m}_{H1}\Delta H_{abs} \end{aligned} \tag{2}$$

with h being the hydrogen specific enthalpy (kJ/kg), M_{MH} and M_W being the mass of each metal hydride material and of the tubing walls (kg), C_{PMH} and C_{PW} being the specific heat of the metal hydride and of the tubing wall respectively (kJ/kg-K), averaged between the absorption temperature and the desorption temperature and ΔH being the metal hydride chemical reaction enthalpy (kJ/kg) during absorption and desorption. The absorption and desorption times are indicated as Δt_{abs} (s) and Δt_{des} (s) respectively.

Equation 2 has been derived making the following assumptions. The heat capacity of the hydrogen absorbed and desorbed in the MH has been assumed negligible compared to the heat capacity of the materials (metal hydride and tubing walls). This is due to the low weight capacity of the materials adopted for the current compression systems, which is typically on the order of 1-2 wt% [Ref]. In addition, the system heat losses have been assumed negligible compared to the other thermal power terms.

The thermal power exchanged between the heat transfer fluid (e.g. pressurized water) and the materials, during absorption and desorption, is expressed as follows. During hydrogen desorption the heating power, available from the EHC system, is provided at (inlet) temperatures of T_{HH1} and is expressed as:

$$\dot{m}_{HH}\overline{C_{PHH}}(T_{HH1} - T_{HH2}) = \frac{(M_{MH}\overline{C_{PMH}} + M_W\overline{C_{PW}})(T_{des} - T_{abs})}{\Delta t_{des}} + \dot{m}_{H2}\Delta H_{des} \tag{3}$$

It is also assumed the mass continuity of the hot utility heat transfer fluid flowing in/out the EHC. Therefore, $\dot{m}_{HH} = \dot{m}_{HH1} = \dot{m}_{HH2}$

During hydrogen absorption the cooling power is provided at (inlet) temperatures of T_{CH1} and is expressed as:

$$\dot{m}_{CH}\overline{C_{PCH}}(T_{CH2} - T_{CH1}) = \frac{(M_{MH}\overline{C_{PMH}} + M_W\overline{C_{PW}})(T_{des} - T_{abs})}{\Delta t_{abs}} + \dot{m}_{H1}\Delta H_{abs} \tag{4}$$

It was also assumed the mass continuity of the cold utility heat transfer fluid. Therefore, $\dot{m}_{CH} = \dot{m}_{CH1} = \dot{m}_{CH2}$

The mass of each MH material can be estimated as:

$$M_{MH} = (\dot{m}_{H1}\Delta t/wt)/\eta_v \tag{5}$$

with $\Delta t = \Delta t_{abs} = \Delta t_{des}$, assuming that the absorption time is equal to the desorption time. The volumetric efficiency factor accounts for the void fraction in the bulk material and for the expansion and contraction of the MH during absorption and desorption respectively.

The values of T_{abs} and T_{des} are assessed as the temperature values corresponding to the equilibrium pressures during absorption and desorption. Their values are estimated using the van't Hoff equation (Equation 6), which is derived from the Gibbs energy expression:

Preprints (www.preprints.org) | NOT PEER-REVIEWED | Posted: 4 June 2018 doi:10.20944/preprints201806.0025.v1

Peer-reviewed version available at Metals 2018, 8, 469; doi:10.3390/met8060469

$$P_{abs} = exp\left(\frac{\Delta H_{abs}}{RT_{abs}} - \frac{\Delta S_{abs}}{R}\right)$$

$$P_{des} = exp\left(\frac{\Delta H_{des}}{RT_{des}} - \frac{\Delta S_{des}}{R}\right) \quad (6)$$

with $p_{abs/des}$ being the equilibrium pressure (bar) values for absorption and desorption. To carry out a techno-economic feasibility study and compare the material performance, the following assumptions were made: (1) the material hysteresis is assumed negligible, thus implying that $\Delta H_{abs} = \Delta H_{des}$ and $\Delta S_{abs} = \Delta S_{des}$ and (2) pressure is used in the van't Hoff expression rather than fugacity, assuming an acceptable error at high pressures as well.

A first conceptual design of the MHC heat transfer system was also carried out. A novel heat transfer system configuration was identified and adopted for the high-pressure scenario. It is comprised of a series of MH material filled tubes. Finned mini-channel cylindrical tubes, located inside the MH tube, provide the required cooling/heating power to charge/discharge the hydrogen. The frontal 2D view of a single tube is shown in Figure 2. The proposed system has several advantages over more traditional heat transfer systems with the heat transfer fluid flowing in the shell side of the component. The wall of the MH tube, in general, can be very thick, given the current operating pressure conditions of 875 bar. Therefore, including an insulation layer between the MH tube and the vessel wall, the proposed solution allows a direct heat exchange between the fluid and the MH material. This avoids the presence of additional relevant thermal inertia represented by the MH tube wall.

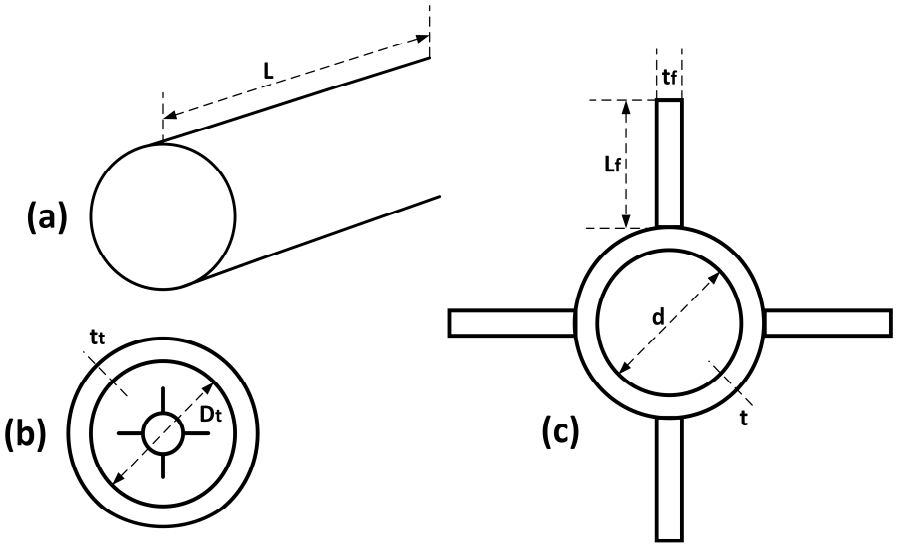

Figure 2. Single tube MH material heat transfer coupled system, showing: (a) Simplified external view of a single MH tube; (b) 2D frontal view of the single tube with 4 fin internal mini-channel heat transfer tube; (c) zoomed view of the internal finned minichannel heat transfer fluid tube.

The steady state heat transfer energy balance equation during hydrogen absorption, using the Log Mean Temperature Difference (LMTD) approach, is expressed as:

$$\dot{m}_{CH}\overline{C_{PCH}}(T_{CH2} - T_{CH1}) = h\, S_{abs}\frac{T_{CH2} - T_{CH1}}{ln\left(\frac{T_{CH2} - T_{abs}}{T_{CH1} - T_{abs}}\right)} \quad (7)$$

The steady state heat transfer energy balance equation during hydrogen desorption, using the LMTD approach, is expressed as:

$$\dot{m}_{HH}\overline{C_{PHH}}(T_{HH1} - T_{HH2}) = h\,S_{des}\frac{T_{HH1} - T_{HH2}}{ln\left(\frac{T_{HH1} - T_{des}}{T_{HH2} - T_{des}}\right)} \quad (8)$$

Constant steady state temperatures during absorption and desorption were assumed. The heat transfer coefficient, accounts for the conductive heat transfer process inside the MH material and the convective laminar heat transfer in the fluid. The overall heat transfer coefficient under laminar conditions can be assessed from Equation 9:

$$\frac{1}{h} = \frac{d\,ln\left(\frac{D_t}{d}\right)}{2\,k_{MH}} + \frac{d}{4.66\,k_{HF}} \quad (9)$$

with k_{HF} and k_{MH} (W/m-K) being the thermal conductivity of the heat transfer fluid and of the metal hydride material respectively.

Equation 9 was derived assuming that the thickness of the heat transfer tubes (t) is negligible and that Nu = 4.66 for the heat transfer fluid under laminar flow conditions [8].

The heat transfer surface area of the heat exchanger is:

$$S = \max(S_{abs}, S_{des}) \quad (10)$$

The mass of the tubing walls is estimated based on the adopted heat transfer configuration as well as on the operating conditions, as discussed in the next sections.

The conceptual design of the material heat exchanger coupled system was carried out based on the geometrical constraints, defined by the heat transfer requirements and the volume occupied by the MH material. The required heat transfer surface area (S) and the volume (V) occupied by the MH material are expressed in Equations 11 and 12:

$$S = N_T(\pi dL + n_f L_f L) \quad (11)$$

$$V = \frac{M_{MH}}{\rho_{bulk}} = N_T\left(\pi\frac{{D_t}^2}{4}L - \pi\frac{d^2}{4}L\right) \quad (12)$$

with N_T and n_f being the overall number of tubes and the number of fins per tube, respectively.

Equations 11 and 12 were derived assuming the thickness of the internal heat transfer tubes (t) and of the fins (t_f) are reasonably negligible compared to the other dimensions.

3.2. Metal hydride compressor system economic model

The installed cost of the MH system was assessed adopting a traditional factored methodology. By this approach the installed cost can be evaluated as the Free on Board (FOB) component cost with additional installation costs, computed using installation factors, as expressed in Equation 13:

$$C_{inst} = f_{inst}C_{FOB} \quad (13)$$

The installation factor (f_{inst}) accounts for the cost of connecting tubing and piping, external insulation, painting, electrical and control equipment, labor, concrete, etc. It also accounts for the high-pressure distribution plates for hydrogen and low-pressure connections for the heat transfer fluid. The values were assessed adopting traditional equipment databases and process modeling programs, namely ASPEN In plant Cost Estimator® [9].

The component FOB cost is expressed as follows:

$$C_{FOB} = C_{MH} + C_{HEPV} \quad (14)$$

The first term (C_{MH}) represents the FOB cost of the MH material. It includes the cost of the raw material, the manufacturing, processing and heat treatment cost and the cost for handling and locating the material inside the tank. This term was assessed based on industrial material data from JMC Alloy [10], for the different selected alloys. The second term (C_{HEPV}) is the FOB cost of the MH tubes and heat exchanger tubing (i.e. finned tubes cost) placed inside the MH tube. The cost of the internal heat transfer tubes was assessed based on industrial tubing values [11], with Al considered

as the constitutive material of the heat transfer tubes. The cost of the MH tubes was assessed based on industrial Swagelok 'Super Duplex' tubing catalogs and from personal communications with Swagelok [12], with SS2507 considered as the constitutive material of MH tubes, operating in a hydrogen environment up to pressures of 900 bar.

4. Results

The techno-economic model was applied to different MH, which were then downselected based upon constraints and initial degrees of freedom assumed on the basis of the compressor configuration and operating conditions. The performance of the selected MHC systems was assessed and compared, showing the potential of selected materials to achieve the required operating conditions.

4.1. Initial downselected materials

To carry out the techno-economic analysis the following assumptions were made. The hydrogen flow rate is between 1 kg/h (for smaller scale applications) and 100 kg/h (for large scale scenarios) based on the DOE targets [1]. With reference to Figure 1, the inlet hydrogen pressure (P_{H1}) is equal to 100 bar, achieved at the exit of the electrochemical stage [3]. The MHC system operates with a compression ratio of 8.75, compressing the hydrogen up to 875 bar, as required by the DOE targets. The MHC system is also assumed to be comprised of a single stage MH compressor, in order to reduce the investment cost and the plant management complexity required by two or multiple stage MH compressors. The MH heating power, required to desorb the hydrogen, is assumed to be provided as waste heat from the EHC at T_{HH1} = 155 °C. The MH cooling power, required to absorb the hydrogen, is assumed to be provided by a cooling source at T_{CH1} = 15 °C. Each of the two MHC system lines (operating in opposite charging/discharging phase) was assumed to be comprised of two MH units operating in parallel, to assure continuity of exercise during possible maintenance or failure of one unit. Some of the degrees of freedom of the problem were assumed *ab initio* limiting the number of the unknows of the overall problem. The charging/discharging time of the MHC was assumed equal to 10 min (i.e. 20 min per each complete cycle), with absence of material weight capacity degradation for (at least) 35,000 cycles. Existing AB_2 MH materials have the right characteristics to achieve the required cycling time (i.e. fast kinetics) and degradation performance [13]. Depending on the formulation, the AB_2 MH material operating pressures can range between 10 bar and over 1000 bar. A comprehensive list of existing AB_2 materials for hydrogen compression applications, both for low and high pressures, can be found in Reference [2]. However, the temperature constraint of the proposed scenario limits the available existing AB_2 metal hydrides to only a few possible candidates. A first screening of the existing AB_2 materials was carried out, based on the available databases and literature data [14,2] and depending on the operating conditions (temperatures and pressures). Four candidate materials were preliminary screened, with their thermodynamic and physical and chemical properties shown in Tables 1-2.

The thermodynamic and weight capacity data for the HP1 material ($TiCr_{1.9}$) were collected from References [15,16]. The corresponding equilibrium operating conditions were estimated using the van't Hoff equation.

Table 1. Thermodynamic properties, weight capacity and equilibrium conditions of the four downselected high pressure metal hydrides (HP1, HP2, HP3, HP4).

Material	$\Delta H_{abs}/\Delta H_{des}$ (kJ/mol$_{H2}$)	$\Delta S_{abs}/\Delta S_{des}$ (kJ/mol$_{H2}$)	wt (%)	Equilibrium P (bar)/ T (°C)
HP1: $TiCr_{1.9}$	26.2	122.0	1.4	100/40 - 875/125
HP2: $(Ti_{0.97}Zr_{0.03})_{1.1}Cr_{1.6}Mn_{0.4}$	23.4	115.0	1.7	100/32 - 875/125
HP3: $Ti_{1.1}CrMn$	22.9	114.7	1.5	100/27 - 875/119
HP4: $TiCrMn_{0.4}Fe_{0.4}V_{0.2}$	20.2/22.0	103.0/109.0	1.9	100/39 - 875/145

Table 2. Chemical and physical properties of the four downselected high pressure metal hydrides (HP1, HP2, HP3, HP4).

Material	ρ_{bulk} (kg/m³)	k_{MH} (W/m-K)	C_{pMH} (J/kg-K)
HP1: $TiCr_{1.9}$	3130	8.0	486
HP2: $(Ti_{0.97}Zr_{0.03})_{1.1}Cr_{1.6}Mn_{0.4}$	3140	8.0	485
HP3: $Ti_{1.1}CrMn$	3170	8.0	493
HP4: $TiCrMn_{0.4}Fe_{0.4}V_{0.2}$	3170	8.0	491

The HP1 material is characterized by significant hysteresis and sloped plateaus at the temperature and pressure range of interest [15,3,17]. Even if the material is characterized by excellent operating pressures and temperatures, it cannot be adopted for an effective high-pressure hydrogen compression system. However, the material was still included as possible candidate material, accounting for possible future material development and modifications to achieve enhanced performance. The HP2 material ($(Ti_{0.97}Zr_{0.03})_{1.1}Cr_{1.6}Mn_{0.4}$) is characterized by flatter plateau profiles and reduced material hysteresis [18]. The thermodynamic and weight capacity data for the HP2 material have been collected from Reference [18], with the corresponding equilibrium operating T and P estimated using the van't Hoff equation. Likewise, the HP3 material ($Ti_{1.1}CrMn$) properties have been assessed based on the data available in Reference [19]. The main limit of the HP3 material is the absorption temperature, required to be on the order of 27 °C for 100 bar. The reduced temperature differences in the heat transfer cooling system makes the design of the heat exchanger more challenging, requiring additional finned structures and higher heat transfer fluid flow rates. The HP4 material thermodynamic properties and weight capacity were collected from Reference [20]. The HP4 material was still included as potential candidate, but is characterized by an operating temperature (145 °C) very close to the hot utility temperature (155 °C), with an overall temperature difference of only 10 °C.

The bulk density was estimated based on the crystal density and assuming a void fraction of 50%. Expansion and contraction of the material during absorption and desorption was assumed equal to 15% of the initial volume under totally desorbed state [2]. The thermal conductivity value was assessed based on the data and information available in References [21-23]. Thermal conductivity values on the order of 5-10 W/m-K are reported when expanded natural graphite is mixed with the material in quantities on the order of about 10wt%. The specific heat values were estimated based on the material formulation, resulting in values on the order of 500 J/kg-K for each material.

4.2. Technical analysis results

The technical feasibility and the corresponding performance of the MH systems comprised of the four downselected alloys are described and discussed in the following sections.

The technical analysis was carried out under the following assumptions. Two scenarios were analyzed: the first scenario saw the adoption of MH compressors for small scale applications (1 kg_{H2}/h, with pressures 100-875 bar), the second scenario was for large scale applications (100 kg_{H2}/h, with pressures 100-875 bar). Given the high-pressure range, only small diameter metal tubes are currently available. The MH tube diameter (D_t) was assumed equal to 1.3 cm, which is the available diameter from Swagelok catalogs, with SS2507 as the constitutive material. The corresponding wall thickness (t_t) was estimated equal to 2.1 mm. This confirms that the optimal heat transfer solution is to include minichannel tubes internally in the MH tubes. Finned aluminum tubes were adopted to transfer the cooling/heating power, with diameter (d) of 2.4 mm. Pressurized water (at pressures of 7.5 bar) was assumed as the heat transfer fluid.

Results in Tables 3 highlight the heating/cooling power required to desorb/absorb hydrogen for 100 kg/h. The contributions of sensible heating/cooling, to vary the operating temperature of the MH bed, and latent heating/cooling required by the chemical reaction (i.e. desorption and absorption respectively) are also shown in the table.

Table 3. Heating and cooling power duty of the four downselected high pressure metal hydrides (HP1, HP2, HP3, HP4) processing 100 kg/h.

Material	Sensible power (kW) [100 kg_{H2}/h]	Reaction power (kW) [100 kg_{H2}/h]	Total power (kW) [100 kg_{H2}/h]
HP1: $TiCr_{1.9}$	130.8	366.8	497.6
HP2: $(Ti_{0.97}Zr_{0.03})_{1.1}Cr_{1.6}Mn_{0.4}$	117.4	327.6	445.0
HP3: $Ti_{1.1}CrMn$	139.2	320.6	459.8
HP4: $TiCrMn_{0.4}Fe_{0.4}V_{0.2}$	127.5[1]	308.0[1]	435.5[1]

[1] The values refer to the desorption phase, which is the most challenging due to the reduced LMTD.

Table 4 shows the results of a first conceptual design of the 4 selected systems.

Table 4. Conceptual design results of the four downselected high pressure metal hydrides (HP1, HP2, HP3, HP4) processing 1 kg/h and 100 kg/h. Each system is comprised of 4 parallel units

Material	Number of tubes[1] [1 kg/h - 100 kg/h]	Number of fins[2] [1 kg/h - 100 kg/h]	Length, L[1] (m) [1 kg/h - 100 kg/h]	Water flow[1] (g/s) [1 kg/h - 100 kg/h]
HP1: $TiCr_{1.9}$	15 - 1474	4 - 4	1.60 – 1.55	28.7 - 2866
HP2: $(Ti_{0.97}Zr_{0.03})_{1.1}Cr_{1.6}Mn_{0.4}$	16 - 1550	4 - 4	1.20 – 1.20	51.3 - 5127
HP3: $Ti_{1.1}CrMn$	14 - 1444	8 - 8	1.60 – 1.50	53.0 – 5297
HP4: $TiCrMn_{0.4}Fe_{0.4}V_{0.2}$	14 - 1565	10 - 10	1.30 – 1.20	62.7 - 6271

[1] per each unit (the system has 4 units)

[2] per each tube

The system design essentially follows a linear relationship with the hydrogen flow rate, from 1 kg/h to 100 kg/h. The sensible heating/cooling power required to increase/decrease the operating temperature plays an important role in the technical performance of the MHC system, contributing for about 26-30% of the overall required thermal power. The reduced temperature differences in the HP4 compressor between the MH and the heat transfer fluid, during the desorption phase (LMTD = 6 °C) results in increased heat transfer surface area (i.e. increase of the number of fins required to transfer the heat during the desorption). Even if the HP4 system requires the lowest heating power (approximately 2% lower than the HP2 material), the reduced LMTD value has also the effect of requiring higher water flow rates (about 22% higher than the corresponding HP2 system) to maintain the heat exchange feasible (temperature pinch point equal to 2 °C).

4.3. Economic analysis results

The economic feasibility and performance of the proposed compression systems are described below. The analysis was carried out using Year 2017 US $. The installation factor, described in Section 3, was estimated adopting ASPEN In Plant Cost Estimator and including additional feasible estimations for the distribution plates. The installation factor values were equal to 1.35 for the large-scale scenario (100 kg/h) and 7.0 for the small-scale scenario (1kg/h).

Results of the small-scale (1 kg/h) and large-scale scenarios (100 kg/h) are shown in Figures 3-4, respectively, highlighting the influence of the MH material cost and the heat exchanger and tubing cost.

Preprints (www.preprints.org) | NOT PEER-REVIEWED | Posted: 4 June 2018 doi:10.20944/preprints201806.0025.v1

Peer-reviewed version available at Metals 2018, 8, 469; doi:10.3390/met8060469

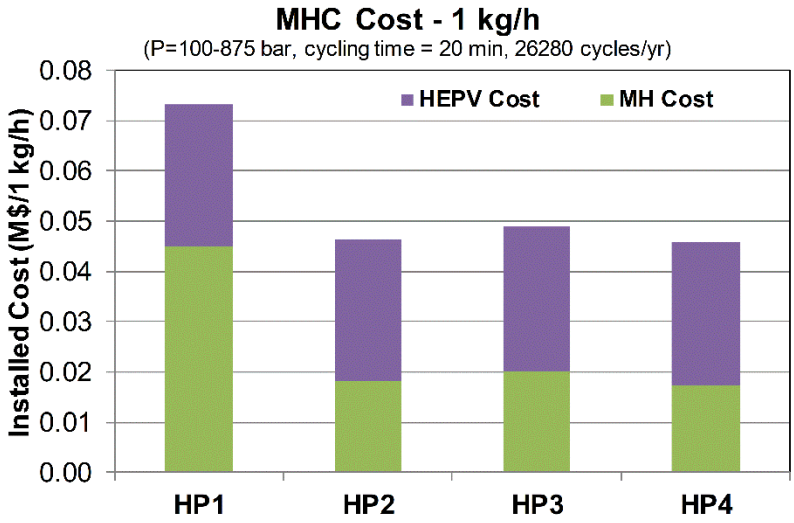

Figure 3. Installed cost of the MHC system for small scale scenarios (i.e. 1 kg_{H2}/h)

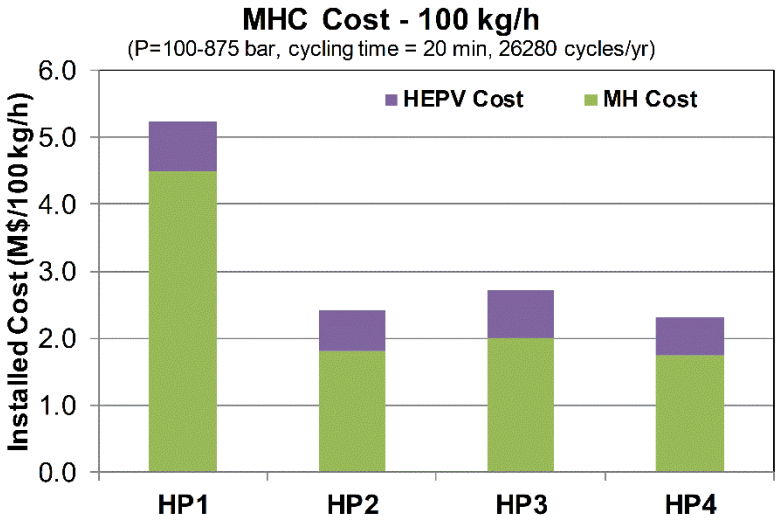

Figure 4. Installed cost of the MHC system for large scale scenarios (i.e. 100 kg_{H2}/h)

The cost of the MH material is directly proportional with the hydrogen flow rate, as for each modular system. The heat exchanger and tubing cost, along with the additional installation costs, follows a power law with regard to the hydrogen flow rate. The HP1 is the most expensive system, mainly due to the MH material cost. For the small-scale scenario, the material cost accounts for about 60% of the overall installed cost. This contribution goes up to about 86% for the large-scale scenario. The HP2 material represents the best option among the selected materials adopted in high pressure systems. For the small-scale scenario the HP2 material cost accounts for about 39% of the overall installed cost, achieving about 75% for the large-scale scenario. The HP3 and HP4 systems have similar performance with the HP2 compressor. The HP3 material cost accounts for about 40% of the overall installed cost for small scale conditions, reaching about 74% for the corresponding large-scale scenario. The HP4 system shows an economic performance essentially identical with the HP2 material. The HP4 material cost influence on the overall small-scale scenario cost is about 40%, reaching values of almost 76% for large scale scenarios.

Cost sensitivity analyses were also carried out for the best candidate material (HP2) at large scale scenarios. The sensitivity analysis 'tornado chart' is shown in Figure 5. Four techno-economic parameters (density, cycle time, material cost and installation cost) were chosen as the most significant quantities.

Preprints (www.preprints.org) | NOT PEER-REVIEWED | Posted: 4 June 2018 doi:10.20944/preprints201806.0025.v1

Peer-reviewed version available at Metals 2018, 8, 469; doi:10.3390/met8060469

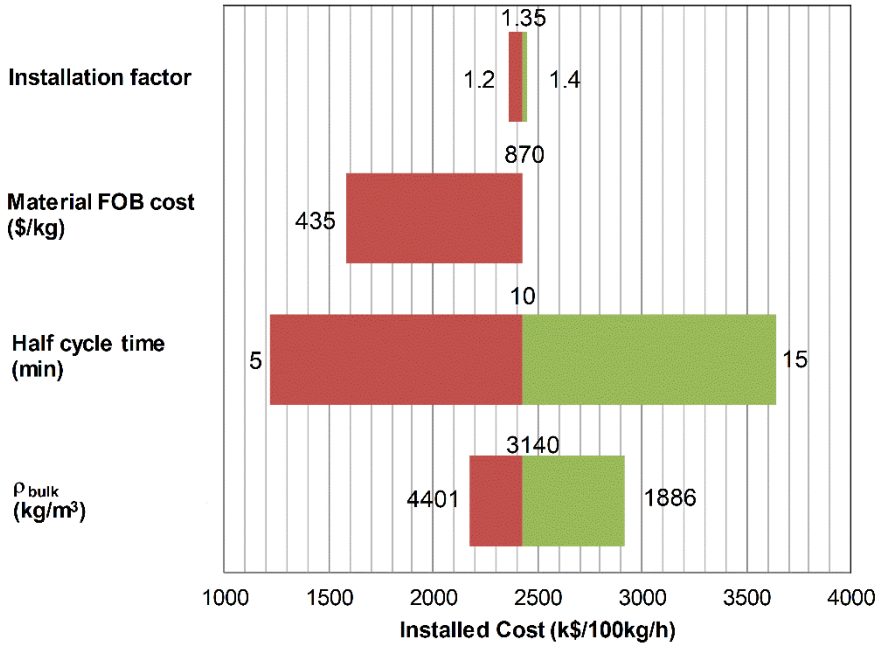

Figure 5. Tornado chart cost sensitivity for the large scale (100 kg/h) HP2 system

Each parameter was varied maintaining constant the other quantities. The heat exchanger system geometry was a fixed parameter for the current sensitivity analysis. The material intrinsic properties (e.g. reaction enthalpy, weight capacity, specific heat, overall thermal conductivity) were also assumed fixed, since their variation would require additional material development and analysis. The bulk material density varied between 30% of the crystal density (i.e. 1886 kg/m^3) and 70% of the crystal density (i.e. 4401 kg/m^3), assuming a different degree of compaction. The baseline bulk density is equal to 3140 kg/m^3, or 50% of the crystal density. The corresponding system cost saw a variation of + 34% with the decrease of the bulk density of about 40% compared to the baseline value. This is also due to presence of additional void space, which reduces the volumetric efficiency of the compressor, resulting in additional metal hydride material to be included in the system. The cycling time is the quantity that showed the highest influence on the overall system cost. A variation of the cycle time of ±50% results in a corresponding cost variation of ±50%, reaching values of about $3.6M for a cycling time of 30 min. A relevant influence on the system cost was also noticed for the MH FOB cost. A reduction of the FOB cost of 50% (i.e. equal to 435 $/kg) resulted in a reduction of the system cost of almost 35%, reaching a value of about $1.6M. The influence of the installation factor on the installed cost was very limited compared to the sensitivity of the other quantities. A reduction of the installation factor from 1.35 (baseline value) to 1.2 resulted in a reduction of the installed cost of approximately 2.7%. The cost of heat exchanger, pressure vessel, distribution plates and installation plays a more relevant role in the small scale scenario (1 kg/h), influencing the overall installed cost for more than 50%.

5. Discussion and future work

Given the stringent constraints dictated by the operating conditions and the need for reduced investment costs, only a few existing MH materials could be downselected as candidates for high pressure MH compressors. Among the four downselected materials only one candidate (HP2 material) has high potential for application in the actual system. The HP1 material is limited by its high slope of the two-phase region and relevant hysteresis, making the hydride not the best candidate for compression applications. In addition, the limited weight capacity and high material cost of the HP1 material result in significant increase of the investment cost compared with the other candidate materials. The HP3 and HP4 materials suffer from the heat transfer management required to achieve pressures between 100 bar and 875 bar. The HP3 hydride requires temperatures lower than 27 °C to

absorb hydrogen at 100 bar making the heat transfer with external cold utility fluid (at 15 °C) challenging. The HP4 material requires temperatures close to 150 °C to desorb hydrogen at 875 bar making the recovery of the available waste heat from the EHC system challenging. The HP2 material will be verified in terms of operating pressures and temperatures at industrial level.

To experimentally evaluate the candidate materials a high-pressure Sieverts' apparatus, reaching pressures > 900 bar, would be designed and built (Figure 6). The system will employ a 2-channel design as to optimize MH characterization. All components will be rated at pressures >1000 bar with minimal volume tubing used to ensure limited dead volume existed between reservoirs and sample holders. The system would be controlled by pneumatically driven valves and regulator allowing for the availability of full automation, thereby, permitting data collection of isothermal, kinetic and cycling measurements. Laboratory cylinder hydrogen would be fed to a flammable gas compressor allowing for the necessary pressures to be achieved for testing. The system would store the compressed hydrogen in a 60-70 ml high-pressure storage container in preparation for aliquots of gas to be absorbed by the sample. The storage reservoir, as well as the channels' reservoirs, would be contained within a temperature-controlled frame. The sample holders would be external from the fame and could be heated or chilled to temperatures ranging from less than -10 to greater than 150 °C. The sample holders chosen would allow for amounts of material >25 g to be tested at a time. Designing the system around large quantities of samples to be measured permits the examination of a prototype-scale level of characterization.

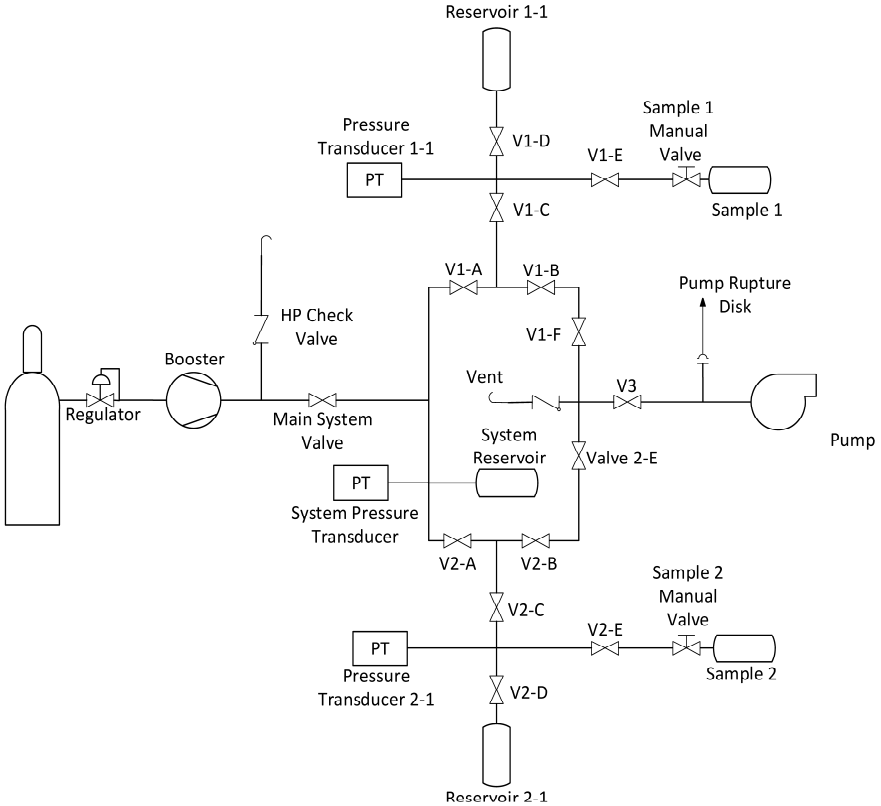

Figure 6. Schematic rendering of a 2-channel high-pressure Sieverts' apparatus for characterization of prototype-scale metal hydride materials.

6. Conclusions

A novel techno-economic analysis model was developed, including steady state mass and energy balance equations, and applied to high-pressure MH thermal compressors. Technical and economic performance of MH systems, compressing hydrogen from 100 bar to 875 bar with heating power provided at temperatures on the order of 150 °C, was assessed. The system was assumed to be coupled with an electrochemical system, which provides the heating power (waste heat from the electrochemical component) required to desorb hydrogen from the metal hydride system. A novel

heat transfer system is also proposed to exchange the heating and cooling power with the metal hydride material. The configuration sees the adoption of finned minichannel heat transfer tubes placed inside the MH material tubes, allowing for enhanced technical performance compared to traditional shell and tube solutions. Only a few metal hydride materials could be initially downselected, being able to achieve the required operating conditions (pressures and temperatures). Results showed that the novel heat transfer system allowed all the downselected materials to potentially achieve the operating pressure (875 bar) at temperatures lower than 150 °C. However only one of the selected alloys, namely $(Ti_{0.97}Zr_{0.03})_{1.1}Cr_{1.6}Mn_{0.4}$ showed more realistic temperature differences in the heat transfer process, making it the best candidate for the proposed application. Cost results, obtained for currently available materials at industrial level for quantities on the order of 10-50 kg, showed the economic feasibility of the proposed system. Economic sensitivity analyses were also carried out, showing different approaches to enhance the economic performance. The overall system cost can be reduced up to about 50% of the initial cost with a reduction of the material cost of 50% and an increase of the bulk density up to 70% of the crystal density.

Author Contributions: The authors contributed as follows: Conceptualization, methodology and results C.C.; Future work, Writing-Review & Editing, M.S.

Funding: The work was carried out under the U.S. Department of Energy Award Number DE-EE0007648.

Acknowledgments: The authors wish to acknowledge Drs. Neha Rustagi, James Vickers and Eric Miller, who are the U.S. Department of Energy managers, for financial support as well as for providing useful comments and direction during the current work. The authors also wish to thank Dr. Robert Bowman Jr. for his insights, help and discussions.

Conflicts of Interest: The authors declare no conflict of interest.

References

1. U.S. Department of Energy Fuel Cell Technologies Office Multi-Year Research, Development and Demonstration Plan - 3.2 Hydrogen Delivery, 2015. https://www.energy.gov/sites/prod/files/2015/08/f25/fcto_myrdd_delivery.pdf (Accessed March 2018).
2. Lototskyy, M.V.; Yartys, V.A.; Pollet, B.G.; Bowman, R.C. Metal hydride hydrogen compressors: A review. Int J Hydrogen Energy 2014, 39(11), 5818-5851.
3. Corgnale, C.; Greenway, S.; Motyka, T.; Sulic, M.; Hardy, B.; Molter, T. et al. Technical performance of a hybrid thermo-electrochemical system for high pressure hydrogen compression. ECS Transactions 2017, 80(10), 41-54.
4. Hattrick-Simpers, J.; Choudhary, K.; Corgnale, C. A simple constrained machine learning model for predicting high-pressure-hydrogen-compressor materials. Mol Syst Des Eng 2018, 10.1039/C8ME00005K, Advance article.
5. Gkanas, E.I.; Grant, D.M.; Stuart, A.D.; Eastwick, C.N.; Book, D.; Nayebossadri, S.; et al. Numerical Study on a Two-Stage Metal Hydride Hydrogen Compression System. J Alloy Compd 2015, 645(1), S18-S22.
6. Karagiorgis, G.; Christodoulou, C.N.; von Storch, H.; Tzamalis, G.; Deligiannis, K.; Hadjipetrou, D.; et al. Design, development, construction and operation of a novel metal hydride compressor. Int J Hydrogen Energy 2017,42(17),12364-12374.
7. Galvis, A.R.; Leardini, F.; Ares, J.R.; Cuevas, F.; Fernandez, J.F. Simulation and design of a three-stage metal hydride hydrogen compressor based on experimental thermodynamic data. Int J Hydrogen Energy 2018,43, 6666-6676.

8. Shah, R.K.; London, A.L. Laminar Flow Forced Convection in Ducts, Supplement 1 to Advances in Heat Transfer; Acedemic, New York, 1978.
9. Aspen In Plant Cost Estimator. ASPEN Tech Manual. Available at https://www.aspentech.com/en/products/pages/aspen-in-plant-cost-estimator (Accessed May 2018) .
10. JMC Alloy. Personal Communication. 2017.
11. Grainger catalog. Available at https://www.grainger.com/category/aluminum-tubing/tubing/pipe-tubing-and-fittings/plumbing/ecatalog/N-qwo (Accessed May 2018).
12. Swagelok catalog. Available at https://www.swagelok.com/downloads/webcatalogs/EN/MS-01-174.PDF (Accessed May 2018).
13. Friedlmeier, G.; Manthey, A.; Wanner, M.; Groll, M. Cyclic stability of various application-relevant metal hydrides. J Alloy Compd 1995, 231(1-2), 880-887.
14. Hydrogen Storage Materials Database http://hydrogenmaterialssearch.govtools.us/search.aspx (Accessed March 2018).
15. Johnson, J.R.; Reilly, J.J.; Reidinger, F.; Corliss, L.M.; Hastings, J.M. On the existence of f.c.c. TiCr1.8H5.3. Journal of the Less Common Metals 1982, 88(1), 107-114.
16. Beeri, O.; Cohen, D.; Gavra, Z.; Mintz, M.H. Sites occupation and thermodynamic properties of the TiCr2-xMnx-H2 (0≤x≤1) system: Statistical thermodynamics analysis. J Alloy Compd 2003, 1-2, 111-122.
17. Corgnale, C.; Hattrick-Simpers, J.; Sulic, M.; Weidner, J.; Lopata, J. Experimental assessment of thin film high pressure metal hydride material properties. Int J Hydrogen Energy 2018, under review.
18. Wang, X.; Chen, R.; Zhang, Y.; Chen, C.; Wang, Q. Hydrogen storage alloys for high-pressure suprapure hydrogen compressor. J Alloy Compd 2006, 420, 322-325.
19. Cao, Z.; Ouyang, L.; Wang, H.; Liu, J.; Sun, D.; Zhang, Q. Advanced high-pressure metal hydride fabricated via Ti-Cr-Mn alloys for hybrid tank. Int J Hydrogen Energy 2015, 40, 2717-2728.
20. Vanhanen, J.P.; Hagstrom, M.T.; Lund, P.D. Combined hydrogen compressing and heat transforming through metal hydrides. Int J Hydrogen Energy 1999, 24, 441-448.
21. Pasini, JM.; Corgnale, C.; van Hassel, B.; Motyka, T.; Kumar, S.; Simmons, K. Metal hydride material requirements for automotive hydrogen storage systems. Int J Hydrogen Energy 2013, 38, 9755-9765.
22. Corgnale, C.; Hardy, B.J.; Tamburello, D.A.; Garrison, S.L.; Anton, D.L. Acceptability envelope for metal hydride-based hydrogen storage systems. Int J Hydrogen Energy 2012, 37(3), 2812-2824.
23. Corgnale, C.; Motyka, T.; Greenway, S.; Perez-Berrios, J.; Nakano, A.; Ito, I. Metal hydride bed system model for renewable source driven Regenerative Fuel Cell. J Alloy Compd 2013, 580(1), S406-S409.
24. Guo, X.; Wang, S.; Liu, X.; Li, Z.; Lu, F.; Mi, J. et al. Laves phase hydrogen storage alloys for super-high-pressure metal hydride hydrogen compressors. Rare Metals 2011,30(3),227-231.

Nomenclature

C	Cost ($)
C_{inst}	Installed cost ($)
C_P	Specific heat (kJ/kg-K)
DOE	U.S. Department of Energy
EHC	Electrochemical hydrogen compressor
f_{inst}	Cost installation factor
FOB	Free on board
h	Specific enthalpy (kJ/kg), or heat trasnfer coefficient (W/m²-K)
k	Thermal conductivity (W/m-K)
LMTD	Log mean temperature difference
$\dot{m}$	Mass flow rate (kg/s)
M	Mass (kg)
MH	Metal hydride
MHC	Metal hydride hydrogen compressor
n_f	Number of fins per tube

N_T	Number of tubes
P	Equilibrium pressure (bar)
R	Gas constant (8.314 J/mol-K)
S	Heat transfer surface area (m^2)
V	Volume (m^3)
wt	Weight capacity (kg_{H2}/kg_{MH})
Greek letters	
ΔH	Reaction enthalpy (kJ/mol_{H2} or kJ/kg_{H2})
ΔS	Reaction enthalpy (kJ/mol_{H2}-K or kJ/kg_{H2}-K)
Δt	Time (s)
η_v	Volumetric efficiency
ρ	Density (kg/m^3)
Subsript	
abs	Absorption
bulk	Bulk
CH	Cold utility
des	Desorption
HEPV	Heat exchanger and pressure vessel
HF	Heat transfer fluid
HH	Hot utility
MH	Metal hydride